

The impact of anti-reflective coating and optical bandpass interference filter on solar cell electrical-thermal performance

Justin C-K Tay¹, Basil T. Wong¹ and Kok-Hing Chong¹

¹ Mechanical Engineering, School of Engineering, Faculty of Engineering, Computing & Science, Swinburne University of Technology Sarawak Campus, Jalan Simpang Tiga, 93350, Kuching, Malaysia
Phone: +6082416353 ext 7942; Fax: +6082260813

ABSTRACT – Solar cells utilize only the visible region of the electromagnetic spectrum to generate electricity. A great reduction in the temperature of a solar cell resulting from filtering infrared and ultraviolet wavelengths will eventually lead to an increase in efficiency. Here, a detailed analysis of the use of an optical bandpass interference filter with antireflective coating as a potential solution to this problem has been carried out. The optical bandpass filter aims to filter out unwanted wavelengths while the antireflective coating functions to reduce the amount of light reflected from the solar panel surface. A simulation program using SolidWorks (Flow Simulation Study) has been performed to demonstrate the effect of utilizing optical bandpass interference filter with antireflective coating on solar panel and the temperature of each cell layer. The thermal analysis results obtained from SolidWorks were then exported to MATLAB/Simulink to investigate the electrical output parameters. Results showed that optical bandpass interference filter combined with antireflective coating could reduce the temperature of the solar cell by 11.83 Kelvin which led to 14.32% increase in the maximum output power within an hour of exposure to peak solar radiation located in Kuala Lumpur, Malaysia.

ARTICLE HISTORY

Received: 18th Apr 2020

Revised: 30th June 2020

Accepted: 14th July 2020

KEYWORDS

Antireflective coating;
SolidWorks simulation;
MATLAB/Simulink
simulation;
optical bandpass
interference filter;
solar cell heat mitigation

INTRODUCTION

In this modern society, people live in a consumer-led and energy extensive society. This has led to a quick depletion of fossil fuels, which is the main source of electricity generation. Fossil fuels compose of coal, natural gas, and oil. They accounted for nearly 64% of the world energy consumption in the year 2014. Although fossil fuels have great potential in generating electricity, these sources are non-renewable as they will deplete once used up. Under current circumstances, oil has a lifespan of 50.7 years, natural gas 52.8 years while coal 114 years [1]. Therefore, it is extremely important to find renewable sources to reduce our dependency on fossil fuels. Solar is the most widely-used renewable energy sources as it is available everywhere in the world. Solar cells only utilize visible light that has a wavelength ranging between 380 to 700 nanometers to generate electricity. Longer wavelengths of more than 700 nanometers do not possess adequate energy to create electron-hole pairs. Shorter wavelengths of radiation such as X-rays do have high photon energies but the high-energy photons could potentially damage the photovoltaic cell through ionization processes. Outside of the visible wavelengths, the undesired radiant energies from the Sun are subsequently converted to heat, causing the solar cell temperature to increase.

It is commonly known that the power output of the solar panel varies significantly depending on the band gap of the cell material as well as the incident radiation wavelength [2]. Ogherohwo et al. [3] attempted an investigation on the effect of wavelength on solar panel. The experiment was carried out using an analytical model to study the performance of the solar cell when different color filters were used. This research proved that visible light region has a greater influence on the performance of a solar panel when compared to all other regions of the solar spectrum. Apart from that, it was observed that among the visible region, red light has the greatest impact on a solar panel as it can lead to the highest output power and efficiency of a panel compared to other regions of visible light (e.g., blue, green, yellow, and orange) [4].

The efficiency of a solar cell drops considerably when the temperature of the solar cell is high [5, 6]. This is due to the facts that high temperature reduces charge carrier mobility, results in electron-phonon scattering as an effect of rising thermal lattice vibrations and weakens the built-in voltage between the p-n junctions. Furthermore, electrons cannot separate from holes effectively due to the affected junction capability. Tobnaghi et al. [7] studies showed that the output voltage has the highest dependency on temperature as it decreased significantly at higher temperature.

Recently, numerous studies have been conducted to demonstrate the use of various optical filtering. Back in 1995, Beachamp and Hart [8] suggested using a solar cell cover, which was then a new invention to block UV and IR rays. This solar cell cover worked by allowing only the visible light region to transmit through it. It consists of several layers of infrared-reflecting coating which aims to remove the low-order reflections and several layers of ultraviolet coating that are found on one or both substrates. These multi-layers can reflect the short (UV) and long wavelengths (IR). The main

advantage of using this technique is that the upper limit of the short wavelength and the lower limit of long wavelength are not interrelated.

Another way of filtering out undesired radiation from the solar cells is using active optical filters to selectively set minimum and maximum allowable wavelengths on the filter [9]. The infrared filter is regarded as the passive filter whilst the ultraviolet filter is considered as the active filter with a tunable cut-off wavelength. However, the method requires tedious calculations to figure out the optimal cut-off wavelength for the active ultraviolet filter. Nonetheless, the optical cut-off wavelength varies significantly throughout the day. Because of these issues, the active optical filters may not be ideal.

In 2014, Roppolo et al. [10] proposed using a cost-effective multifunctional coating which possesses hydrophobic properties besides being able to reflect IR rays. This multifunctional coating used in the study was made of UV-curable epoxy. It was found that the use of this coating did not have any impact on the photo-curing rate. The experiment proved that this coating was a perfect filter in the NIR region from an evaluation of UV-VIS-NIS spectroscopy. By blocking the IR rays from the electromagnetic spectrum, the working temperature and the amount of heat absorbed can be minimized. However, the presented results were limited to only the change in temperature of the solar cell without details on the resulting electrical parameters.

The use of color filters to block radiation with undesired wavelengths has been studied by Gouvêa et al. [11]. A color filter was applied each time to filter out the unwanted wavelengths. Eight color filters were used in the study. Although the use of monochromatic filters was helpful in reducing the cell temperature, it absorbs other solar radiation outside of the specific wavelength particularly in the visible region [12]. This then reduced the electrical power output of the solar cell. The positioning of the filter could also result in heat-trapping issues inside the solar cell since the inserted monochromatic filter may also prevent heat from flowing out of the cell.

Antireflective coatings are well-known to be effective in trapping light inside the photovoltaic cells. Ho et. al [13] conducted an experiment to compare the conversion efficiencies of a single-junction GaAs Solar Cells coated with antireflective layers of Silicon dioxide (SiO_2), Indium Tin Oxide (ITO), and hybrid layer of SiO_2/ITO . The antireflective layer was applied through Radio Frequency (RF). In this experiment, the ITO film was discovered to have the highest conversion efficiency due to a lower series resistance and a higher short-circuit current-density. The ITO film has a refractive index of 2.0 [14] which helped in enhancing the antireflective properties. Furthermore, it was also observed that the ITO film can be easily adhered to the silicon cell [15]. Kishore et al. [16] also suggested an alternative material in silicon nitride as the antireflective coating. The silicon nitride was deposited onto the silicon solar cell by Plasma Enhanced Chemical Vapour Deposition (PECVD). This experiment showed that the short circuit current output had an improvement of nearly 28%. Manufacturing of the solar cell requires high temperature in gas ambient, which causes the formation of the thin oxide layer [17]. This layer makes the optimization of the coating complicated. Kishore et al. [16] also proposed the method of adding silane and the nitrogen gas mixture to the silicon nitride film to increase its refractive index.

In order to simulate the photovoltaic panel, details such as weather data that include irradiance and temperature are required [18]. These data represent the input test condition. In this study, the results obtained from the simulation were current, voltage and power, which were highly responsive to the changes in the input. The relationship between irradiance and temperature of the photovoltaic cells was studied using a single diode panel with resistors connected in series and parallel in MATLAB/Simulink. Paul et al. [19] suggested that the effects of irradiance and temperature were investigated and analyzed separately to determine the factor that has a higher influence on the performance of the solar cells. The most reliable method to obtain the parameters at Standard Test Condition (STC) is the Newton-Raphson method [20]. The results yielded were then compared with the theoretical results through manual calculation.

Here, our main objective is to assess the impact of anti-reflective coating and optical bandpass interference filter on solar cell electrical-thermal performance under the optimal configuration. This is achieved by implementing a filtering layer for selectively filter out the undesired radiant energies with wavelengths outside the visible region. An antireflective coating is also used in conjunction with the filtering layer to maximize the conversion efficiency. Once the best configuration is set up, the actual impact of the additional layers on the cell electrical-thermal performance is studied in detail including using the real-time weather conditions to accurately understand how the excessive heating on the solar cells plays a critical role in limiting peak conversion efficiency.

METHODS AND MATERIALS

Determination of the Optimal Thickness of Antireflective Coating

The chosen material for the antireflective coating is titanium dioxide (TiO_2). There are several methods that can be used to deposit the coating onto the glass panel. Some of the common methods are spraying, spin-on, screen printing, and chemical vapor deposition (CVD) [21]. Among these methods, spin-on is the most cost-effective and simple, however, it is not suitable to be applied onto a rough surface. Therefore, titanium dioxide is applied to the panel through screen printed technique in this research. In real-life, Tetraethylorthotitanat ($\text{C}_2\text{H}_5\text{O})_4\text{Ti}$) was deposited onto the panel at about 280°C in the form of TiO_x films. Purified air functions as the carrier gas in the procedure. The coating used should meet the following requirements:

1. The coating must be stable. The material properties should not change when there is a change in temperature and humidity. A good coating must also resist corrosion and oxidation from the atmosphere.
2. The coating should easily and strongly adhere to the surface of the solar panel, so that it remains attached to the panel for a long period of time.
3. The coating should have a long lifespan despite being exposed to elevated temperature repeatedly.
4. The coating must be able to reduce the reflection of light so that more light can be concentrated onto the optical bandpass interference filter.

It is important to calculate the suitable thickness of the antireflective coating for the metallization process of electrical contacts. An overly-thick antireflective coating may complicate the process of pad metallization, thus leading to a decrease in the efficiency of the solar cell. According to the Fresnel equations, the reflection coefficient of the coated surface can be calculated using the following equation [15],

$$R = \left[\frac{(n_c^2 - n_1 n_2)}{(n_c^2 + n_1 n_2)} \right]^2 \quad (1)$$

where n_c is the refractive index of coating, n_1 the refractive index of medium, n_2 the refractive index of substrate. The main aim of the antireflective coating is to reduce the reflection of sunlight on the surface of the solar panel. Thus, in an ideal case, the reflection coefficient (R) is 0. This will lead to the equation of,

$$n_c = \sqrt{n_1 n_2} \quad (2)$$

To obtain the required thickness of the Titanium Dioxide (TiO_2), the following equation is used,

$$t_c = \frac{\lambda_0}{4n_c} \quad (3)$$

where λ_0 is the wavelength in the range of 400-1100 nm.

Selection of Optical Bandpass Interference Filtering

Optical bandpass interference filter has been chosen as the solution to the problem underlined in this work. Two most common types of the optical filter are absorption filter and interference filter. Interference filter is preferred here as it can cancel out the unwanted wavelengths and reflects the heat energy back to the surrounding. This can greatly reduce the temperature on the solar panel as less heat is trapped between the solar cell and the optical filter. Unlike interference filter, absorption filter works by absorbing heat from the selection of wavelengths, which leads to hotter film. The parameters to be considered in the selection of optical filter are the thickness, size, and permitted wavelengths.

It is important that the optical filter should be as thick as possible. A thicker optical filter is much more efficient in filtering ultraviolet rays and infrared rays. This can be explained as the light from the sun has to travel a longer distance before reaching the solar cell. The size of the optical filter should be of the same size or larger than the solar panel. A smaller size of the optical filter should be avoided because a small-sized optical filter is not capable of reducing the unwanted wavelengths effectively throughout the entire panel. Lastly, the permitted wavelength should range between 390 nm to 700 nm which falls between the visible region.

To determine the best optimal cut-on and cut-off wavelength that allows only visible light to pass through, the equations below are used. The information of the Full Width Half Maximum (FWHM) and Centre Wavelength (CWL) can be found in manufacturer's datasheet.

$$\text{Full Width at Half Maximum (FWHM)} = \lambda_2 - \lambda_1 \quad (4)$$

$$\text{Center Wavelength (CWL)} = \frac{\lambda_2 - \lambda_1}{2} \quad (5)$$

Solar Panel Design

The structure of the studied solar panel is illustrated in Figure 1 and Figure 2. Bandpass interference filter has been chosen as its range of allowable wavelengths matches the visible region which is 435 nm - 720 nm. Thus, the filter enables the visible light wave to pass through the panel whilst blocking the longer wavelengths (infrared) and shorter wavelengths (ultraviolet rays). The shape of the optical filter is rectangular and is to be positioned directly above the solar panel instead of 1 cm or 2 cm above the solar panel to prevent heat-trapping issues. The antireflective coating is then applied directly onto the top of the optical bandpass interference filter.

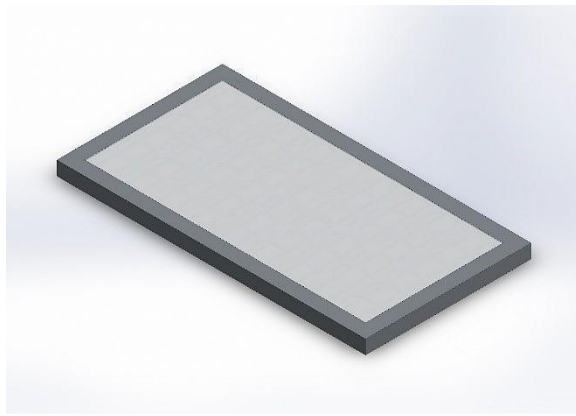


Figure 1. Schematic of the panel design.

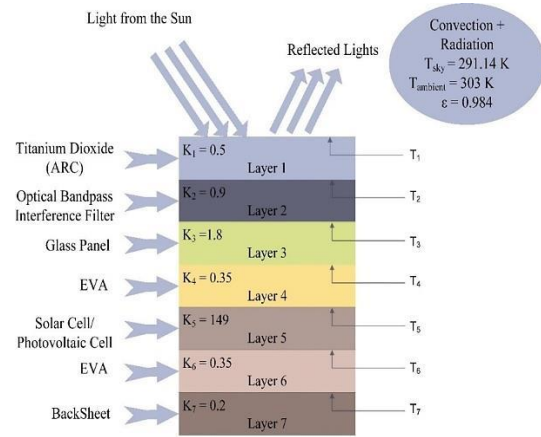


Figure 2. Overall setup of each layer.

Heat Transfer

Since the primary research aim is to improve the efficiency of the solar cell by blocking the unwanted wavelengths, the main interest of the project is to calculate and simulate the temperature of the cell and assess the impact on the cell performance. To calculate the temperature of the cell, it is important to employ the thermodynamic principles such as convection, radiation, and conduction. In this simulation, the heat generated from the solar cell is assumed to be equal to the heat released to its surroundings, therefore the system is in thermal equilibrium. The temperature of each layer is then verified through simulation using SolidWorks (Flow Simulation Study). Both panels to be tested in the simulation possess similar settings such as the weather conditions, material properties, and duration of exposure to the sun. This is particularly important as a slight difference in the setting can affect the accuracy and reliability of the results. Both solar panels are simulated to be under the sun for one hour, from 2 p.m. to 3 p.m. The temperature of each layer is then recorded and analysed.

A few assumptions were made when accounting various heat transfer modes. All the assumptions made was based on the Air Mass 1.5 (AM1.5) standard.

- Heat transfer takes place in one dimension. The transfer is assumed to take place in only a single direction, the heat transfer in other directions is treated as negligible.
- The system is treated to be in steady state. Therefore, the properties of the materials remain constant throughout.
- The surrounding temperature is taken to be 30°C (303 K).
- The temperature and emissivity of the sky are found using the equations below [22],

$$T_{sky} = 0.0552T_{air}^{1.5} \quad (6)$$

$$\varepsilon_{cloud} = (1 - 0.84CC) \left(0.527 + 0.161e^{8.45 \left(1 - \frac{273}{T_{air}} \right)} \right) + 0.84CC \quad (7)$$

where CC is Cloudiness 1[cloud sky] & 0[clear sky], T_{sky} is sky temperature, T_{air} is air temperature and ε_{cloud} is cloud emissivity.

- The convection which occurs at the top layer and bottom layer of the solar cell are taken to be natural convection.
- The thickness of the antireflective coating is regarded as negligible due to its small value.

A 'Flow Simulation Study' is selected to simulate the temperature of each layer as a result of the three modes of heat transfer (conduction, convection and radiation). A detailed calculation and the boundary conditions of each layer will be discussed below. The convection that takes place on the top and bottom layer of the solar cell is assumed to be natural convection. Natural convection refers to the flow that is initialized by the difference in the density of the fluid, unlike forced convection which requires an external source such as fan or pump to initiate the flow. The equations used to calculate the convection heat transfer coefficient due to natural convection [23] are shown below:

$$T_f = \frac{T_s + T_\infty}{2} \quad (8)$$

$$\beta = \frac{1}{T_f + 273} \quad (9)$$

$$L_c = \frac{A_s}{P} \quad (10)$$

$$Ra_L = \frac{g\beta(T_s - T_\infty)L_c^3}{\nu^2} Pr \quad (11)$$

$$Nu = 0.54 Ra_L^{\frac{1}{4}} \quad (12)$$

$$h = \frac{Nu * k}{l} \quad (13)$$

$$\dot{Q}_{convection} = hA_s(T_s - T_\infty) \quad (14)$$

where,

T_f	= Film temperature (K)
T_s	= surface temperature (K)
T_∞	= ambient temperature (K)
B	= coefficient of volume expansion (1/K)
L_c	= distance (m)
P	= parameter (m)
R_{al}	= Rayleigh number
G	= gravity acceleration
Pr	= Prandtl number
ν	= kinematic viscosity of the fluid (m ² /s),
Nu	= Nusselt Number
h	= convection heat transfer coefficient (W/m ² K)
k	= thermal conductivity (W/mK)
A_s	= cross sectional area
$\dot{Q}_{convection}$	= rate of convection heat transfer

Conduction refers to heat transfer through collision of the molecules of a higher kinetic particle with a less kinetic particle [23]. Heat conduction takes place on all layers. To simulate this process on SolidWorks, all the materials must be assigned carefully, and the thickness and thermal properties of each layer should be set as in Table 1.

$$\dot{Q}_{conduction} = \frac{-kA\Delta T}{\Delta x} \quad (15)$$

where,

A	= cross sectional area
ΔT	= difference in temperature (K),
Δx	= the length difference
$\dot{Q}_{convection}$	= the rate of conduction heat transfer

Considering radiation in the solar cell, the emissivity of each layer must be known. The emissivity of the layers is shown in Table 2 [24].

$$\dot{Q}_{radiation} = \varepsilon\sigma A_s(T_s^4 - T_{surrounding}^4) \quad (16)$$

where,

ε	= emissivity
σ	= Stefan-Boltzmann Constant ($\text{W/m}^2\text{K}^4$)
$T_{\text{surrounding}}$	= surrounding temperature (K)
$\dot{Q}_{\text{radiation}}$	= rate of radiation heat transfer

Table 1. Thermal conductivities and thickness of each layer

Component in Solar Cell	Thickness (mm)	Thermal Conductivity, k (W/m-K)
Titanium dioxide (ARC)	0.0013	0.5
Optical Bandpass Antireflective Coating	3	0.9
Glass Panel	3.2	1.8
Ethylene Vinyl Acetate (EVA)	0.45	0.35
Silicon Solar Cell (P-N junction)	0.4	149
Backsheet	0.2	0.2

Table 2. Emissivity (ε) of some layers. [24]

Description	ε
Glass	0.90
Sky	0.98
Ground	0.93
Back sheet	0.86

Setting of Simulation (Thermal – Flow Simulation)

A wind speed of 1.5 m/s in x-direction is taken into consideration for convection heat transfer. In the simulation involving a solar panel that has an optical bandpass interference filter with antireflective coating, it is important to add and edit a custom material because SolidWorks Library does not provide the selection of any optical filter related materials or components.

Thus, the optical filter must be added manually into the SolidWorks Library. The specifications of the components can be obtained from the manufacturer's datasheet. The thickness of the antireflective coating (Titanium Dioxide) is relatively small and is regarded as negligible in the drawing of each part. Thus, it is assumed that Titanium Dioxide is directly coated onto the optical bandpass interference filter. However, in setting the material of the optical bandpass interference filter, it is highly critical to adjust the refractive index to 2.6 of TiO_2 to be able to show the effect of the antireflective coating. Figure 3 shows the transmission data of the optical bandpass interference filter used in this work. It is stated in the manufacturer specification that the thickness tolerance for 575WB350 is ± 0.1 mm.

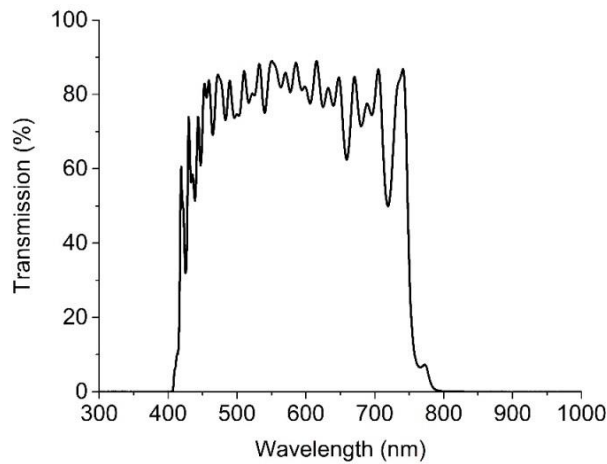


Figure 3. Transmission data of the optical bandpass interference filter used in the simulation (575WB350)

Table 3. Parameters and characteristics of the solar cell

Parameters	Values
Rated Maximum Power, P_{mp} (W)	250
Rated Maximum Current, I_{mp} (A)	8.65
Rated Maximum Voltage, V_{mp} (V)	28.81
Short-Circuit Current, I_{sc} (A)	9.21
Open Circuit Voltage, V_{oc} (V)	35.42
Series Resistor, R_s (Ω)	0.221
Shunt Resistor, R_{sh} (Ω)	415.405
Ideality factor of diode, n	1.3
Number of cells connected in series, N_s	54

MATLAB (Simulink)

Simulink is an extension of MATLAB which was developed to model, simulate and analyse multi-domain dynamical system. It encompasses a library that has a wide variety of components. Simulink is closely linked to MATLAB and the results obtained using this extension system can easily be exported to MATLAB. Furthermore, Simulink is commonly used in the field of automatic control and digital signal processing. In Simulink, sets of blocks were used to build a model of solar panel to simulate the electrical parameters of the solar panel. Before creating the solar panel model, the characteristics of the solar cell were determined either from the datasheet or manufacturer's brochure. Different solar cell has distinct values for each parameter. To assess the effect of adding the designed layer, the electrical parameters of the modified panel are compared with that of a conventional panel. To ensure the modification is the only independent variable in this relationship study, both solar panels tested must have identical characteristics and parameters. In the setup of the panels, the characteristics in Table 3 were followed.

To study the electrical behavior of a photovoltaic cell, it is important to have an equivalent circuit which is based on discrete ideal electrical components. To simplify this study, a photovoltaic cell is modelled as a current source that is connected in parallel with a diode as shown in Figure 4. Since there are always some losses in the form of resistance, an ideal solar cell does not exist. Therefore, to compensate for these losses, a shunt resistor and a series resistor are included in the circuit.

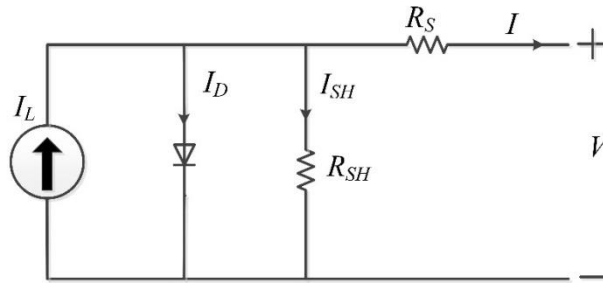


Figure 4. Equivalent circuit of solar cell

The amount of solar radiation absorbed by a solar collector can be calculated using Eq. (17). Using this equation, the amount of heat formed on the surface of the top layer can also be identified as:

$$P = G_n \cdot A - G_{rif} \cdot A \quad (17)$$

where G_n is the solar irradiance collected on the solar panel, G_{rif} is the irradiance reflected from the solar panel and A is the surface area.

Some electrical parameters such as maximum output power, short circuit current and open circuit voltage obtained from running simulations using SolidWorks and MATLAB were used to calculate the efficiency of both solar cells, through relating the following equations,

$$I_{ph} = [I_{sc} + k_i * (T - 302)] * \frac{G}{1000} \quad (18)$$

$$I_{rs} = \frac{I_{sc}}{e^{\left(\frac{qV_{oc}}{n * N_s * K * T}\right)} - 1} \quad (19)$$

$$I_o = I_{rs} * \left(\frac{T}{T_n}\right)^3 * e^{\left(\frac{q * E_{go} * \left(\frac{1}{T_n} - \frac{1}{T}\right)}{n * K}\right)} \quad (20)$$

$$I_{sh} = \frac{V + (I * R_s)}{R_{sh}} \quad (21)$$

$$I = I_{ph} - (I_o * [e^{\left(\frac{qV_{oc}}{n * N_s * K * T}\right)} - 1]) - I_{sh} \quad (22)$$

where,

I_{ph}	= photocurrent (A)
k_i	= short circuit current of cell at 25 °C and 1000 W/m ²
T	= operating temperature (K)
G	= solar irradiation (W/m ²),
I_{rs}	= reverse saturation current (A),
Q	= electron charge (C)
K	= Boltzmann's constant (J/K)
I_o	= reverse saturation current (A)
T_n	= nominal temperature (K)
E_{go}	= band gap energy of the semiconductor (eV),
I_{sh}	= shunt resistor current (A)
I	= output current (A)

The electrical model is then used to calculate the I-V characteristic of the design taking into consideration the maximum temperature of the cell with the additional of the ARC and filtering layers. The solar panel model based on the SolidWorks drawing is created in Simulink to simulate and predict the associated electrical characteristics. The solar panel block in Simulink is shown in Figure 5.

Overview of the entire solar panel

The simulated temperatures of both the conventional and modified panels are entered in the temperature section. The solar irradiance is set according to the actual amount of irradiance that will be used in the conversion to electrical energy. The solar irradiance that will be used in the conversion can be obtained from SolidWorks simulation by creating a surface goal on the solar cell. Both solar panels will be studied with an assumption that the surface is clean from dust. This is exceptionally important as dust will lead to a loss in incident solar radiation [25]. The solar irradiance for this case is set to be constant with 1056 W/m^2 . After running the program, the I-V and P-V curves for each condition are then plotted either by manually typing the script in MATLAB or automatically using the X-Y curve in Simulink. The voltage sensor, current sensor and power sensor are used to read the values of voltage, current and power respectively. The electrical parameters as tabulated in Table 3 are entered into the Initial Function of Simulink after all the models have been finalized.

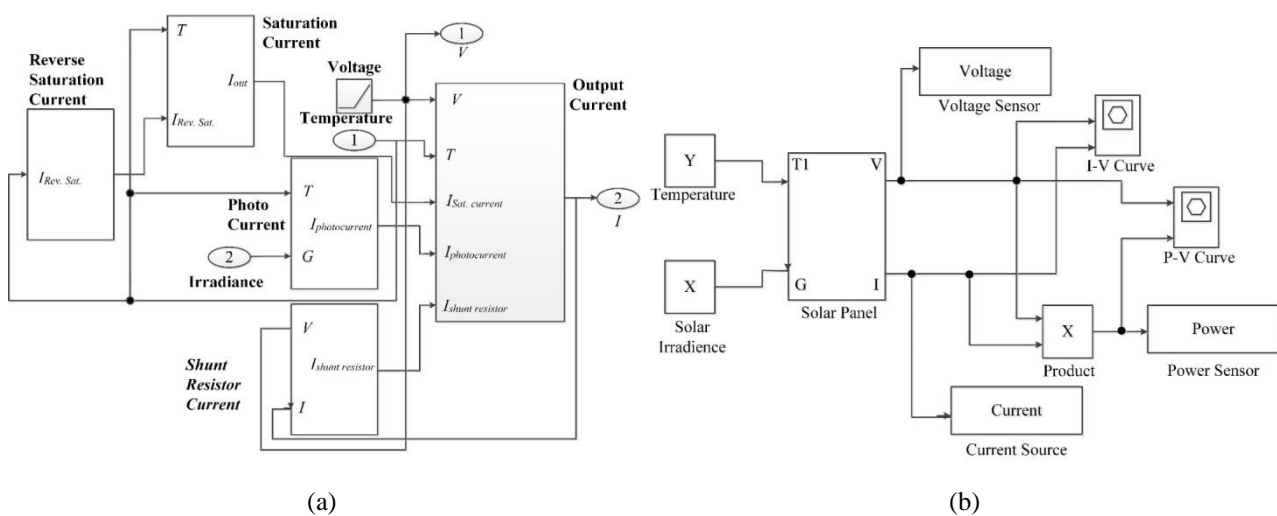


Figure 5. (a) Solar panel blocks in Simulink and (b) Overall model of solar cell

Fill factor

Fill factor is a method commonly used to identify the overall behavior of photovoltaic cells and the quality of a solar cell. Fill factor is determined as the ratio of the maximum output power produced by the solar cell to the product of short circuit current and open circuit voltage. Its value is affected by several factors such as the shunt resistances, number of cells connected in a series and the losses due to the diode. By lowering the series resistance and increasing the shunt resistance, fill factor can be increased. The higher the fill factor, the more efficient is the solar cell. Theoretically, the fill factor of most solar cell ranges from 50% to 82%. In this research, the maximum output power is obtained when the solar panels were at their highest temperatures when placed under simulation with a real-time of 2 p.m. to 3 p.m.

RESULTS

Several simulations have been carried out to illustrate the effectiveness of optical bandpass interference filter with antireflective coating in reducing the cells temperature.

Mesh Convergence Study

A mesh independence study is carried out to study the relationship between the simulated results and the level of mesh. There are 7 levels of meshes for Flow Simulation. To study the results for different mesh level, mesh level of 1 (69,897 cells), 4 (1,365,590 cells) and 6 (6,877,882 cells) are used in simulating the Conventional panel (without optical bandpass interference filter & anti-reflective coating). The maximum and minimum temperature of the silicon cell only differs slightly between each level of mesh as shown in Table 4. Since running a simulation process with a high level of mesh is rather time-consuming, the simulation is allowed to run with a mesh level of 1 for all different type of tests performed in this paper.

Table 4. Minimum and maximum temperature of silicon cell with different mesh level

Mesh Level	Temperature of Silicon Cell (K)		
	Level 1	Level 4	Level 6
	68,897	1,365,590	6,877,882
Minimum temperature	302.96	302.75	302.57
Maximum Temperature	324.06	324.31	324.50

Flowchart

The overall solution procedures in the methodology is depicted in a flowchart as shown in the Figure 6.

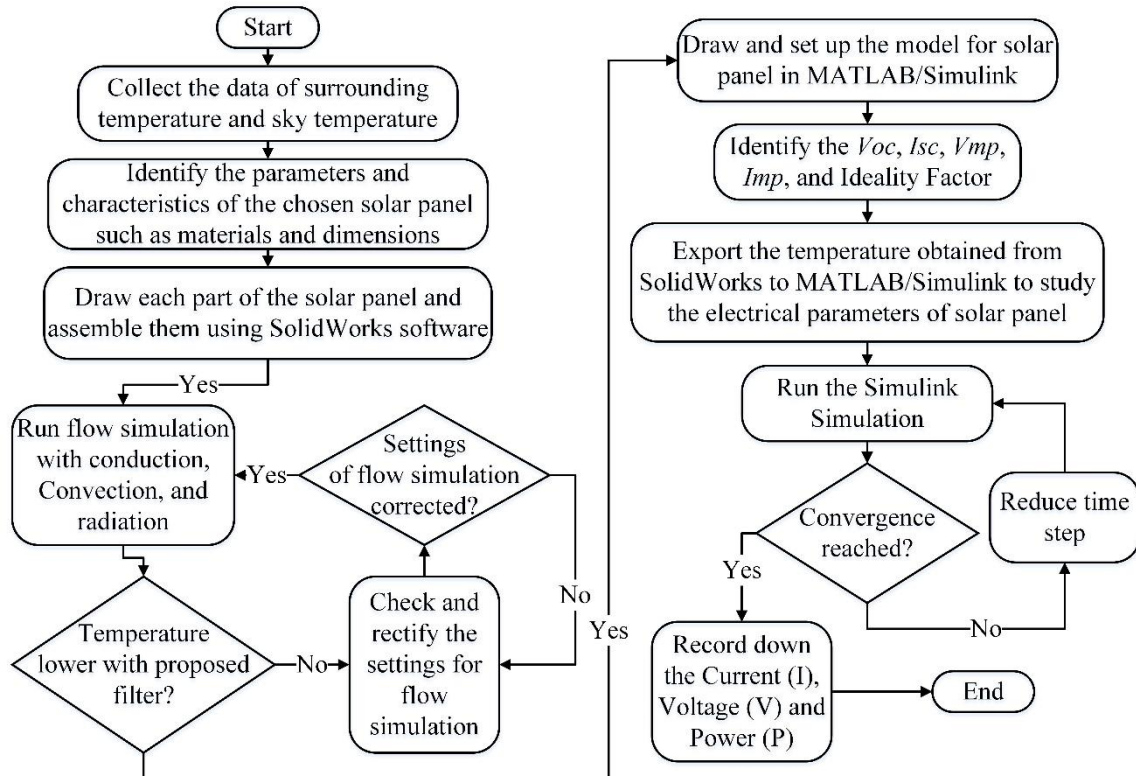


Figure 6. The methodology flowchart summarizes the solution approach in this work

Thickness of Optical Bandpass Interference Filter with Antireflective Coating

Thickness plays an important role in controlling the amount of light being transmitted. Here, a solar cell with a 1-mm thick filter is compared against one with a 3-mm thick filter in terms of the filtering effect and the cell temperature variation. As shown in Table 4, the temperature is slightly lower when a thicker (i.e., 3 mm) designed layer was used. This phenomenon can be explained by the longer distance that has to be travelled by heat to reach the P-N junction. Generally, a thicker optical filter is more efficient in blocking light and heat. The selection of the thickness of optical filter should also take into consideration the trade-off between its cost and effectiveness. In this study, the temperature variation between solar cells using the 1-mm and 3-mm thick optical filters is only 0.36°C, which is negligible.

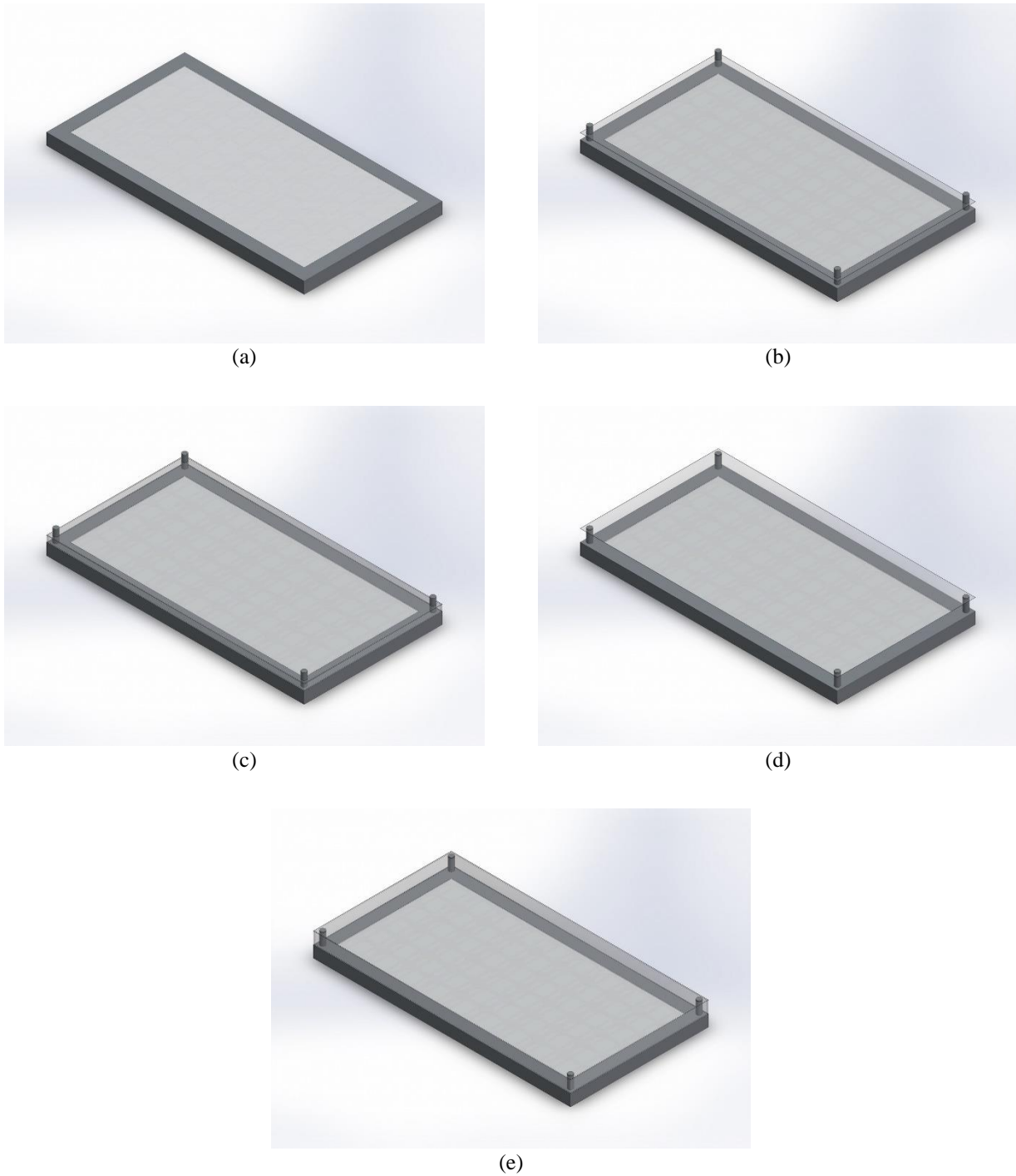


Figure 7. Solar panel with a gap distance between the filter and the PV layers of (a) 0-mm, (b) 25 mm, (c) 25 mm with full cover on sides, (d) 50 mm and (e) 50 mm with full cover on sides

Table 5. Effect of optical bandpass interference filter thickness on maximum cell temperature

Time (s)	Filter Thickness 1 mm	Filter Thickness 3 mm
0	300.00	300.00
600	303.96	303.85
1200	306.65	306.46
1800	308.76	308.50
2400	310.39	310.09
3000	311.64	311.31
3600	312.59	312.23

Filter Distance from the Glass Panel of PV Cell

After selecting the optimum thickness of the designed layer, the ideal distance between the optical filter with antireflective coating and the solar panel (i.e., the gap distance between layers 1-2 and 3-7) is examined next. Five different design scenarios (i.e., 0 mm, 25 mm, 25 mm with full cover on sides, 50 mm, and 50 mm with full cover on sides) are considered in the simulations and the results are analyzed to investigate the electrical-thermal impact of the filter on the solar cell. To better illustrate these different configurations, the physical appearances of each consideration from (a) to (e) are depicted in Figure 7.

Based on the simulation results, it is observed that in general the shorter the gap distance between the optical filter with antireflective coating and the solar panel is, the lower the maximum temperature is in the solar cell panel. Hence, careful planning is required when placing the optical bandpass interference filter at a distance away from the solar panel. With a gap distance established between the filter and the solar panel, air that is sandwiched within the distance reduces potential heat loss via convection and conduction through the other cell layers. As a result, an overall increase in the temperature of the solar panel over time is observed. In addition, placing the optical filter at a distance away from the solar panel leads to the possibility of having other electromagnetic spectrum such as infrared and ultraviolet rays penetrating through the sides, which then directly heat up the cell. As evident in Table 5, the cell temperature is generally lower when a full cover is used compared to those without full cover. Hence, it is best when the filter is in full contact with the glass layer of the solar cell. Not only this makes the overall solar panel compact but also it lowers the impact of excessive heating on the cell which may lead to a lower conversion efficiency. This can be evident from the P-V and I-V curves computed (see Figure 8) where more electric current (thus power) can be generated at voltages more than 20 V when there is no gap distance between the filter and the solar cell itself. This is mainly attributed to findings that there is a noticeable 5 °C different between (a) and the rest of the configurations after exposing to the solar radiation for an hour. For the sake of simplicity, the subsequent analyses in this work are based on the optical filter of 3 mm thick, and it is placed directly above the solar panel (0 mm).

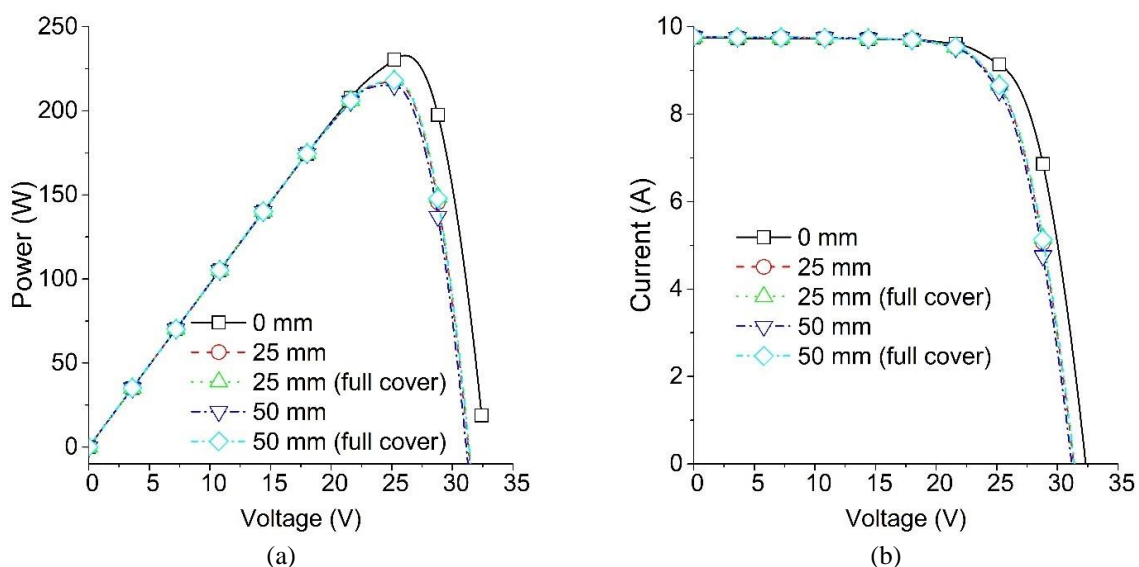


Figure 8. (a) Power-Voltage and (b) Current-Voltage relationship as a function of distance of the optical bandpass interference filter with antireflective coating and solar panel

Cloudy Against Clear Day

In this section, the impact of the ARC coating and the optical bandpass interference filter on the cell electrical-thermal performance is assessed. Three different weather conditions are considered here: clear sky, half- cloudy sky, and full-cloudy sky. These results are shown in Table 6 and Figure 9. It is understood that weather condition plays an important role in governing the electrical power output from the solar cells. On cloudy days, the optical bandpass interference filter with antireflective coating does not achieve its maximum function as demonstrated in the simulated results whereby the cell temperature, P-V curves, and I-V curves start to converge into single curves with and without the coating and filter as the sky goes from half-cloudy to full-cloudy. This is because most light rays from the sun are blocked by the clouds before reaching the solar panel under those weathers. During days with clear sky, it is evident that the implementation of the combined coating and filter produces higher electrical current and power output beyond a voltage of 20V in the cell.

Table 6. Maximum cell temperature for solar panel with antireflective coating and optical bandpass interference filter (3 mm thick) for various gap distances between the filter and the top layer of glass of the PV cell

Time (s)	Distance				
	0 mm	25 mm	25 mm (Full Cover)	50 mm	50 mm (Full Cover)
0	300.00	300.00	300.00	300.00	300.00
600	303.85	304.83	304.72	305.09	304.89
1200	306.46	308.58	308.41	308.99	308.51
1800	308.50	311.68	311.47	312.19	311.61
2400	310.09	314.19	313.93	314.82	314.08
3000	311.31	316.23	315.88	316.92	316.07
3600	312.23	317.84	317.55	318.61	317.63

Table 7. Comparison of temperature based on the use of optical bandpass interference filter on different weather condition

Type	Without Filter			With Filter		
Weather Time (s)	Clear	Half-Cloudy	Full-Cloudy	Clear	Half-Cloudy	Full-Cloudy
0	300.00	300.00	300.00	300.00	300.00	300.00
600	306.72	303.11	299.96	303.85	301.72	299.66
1200	311.81	305.45	299.08	306.46	302.89	299.38
1800	315.96	307.35	298.71	308.50	303.84	299.15
2400	319.29	308.88	298.38	310.09	304.62	298.95
3000	321.94	310.11	298.11	311.31	305.23	298.78
3600	324.06	311.09	297.86	312.23	305.71	298.65

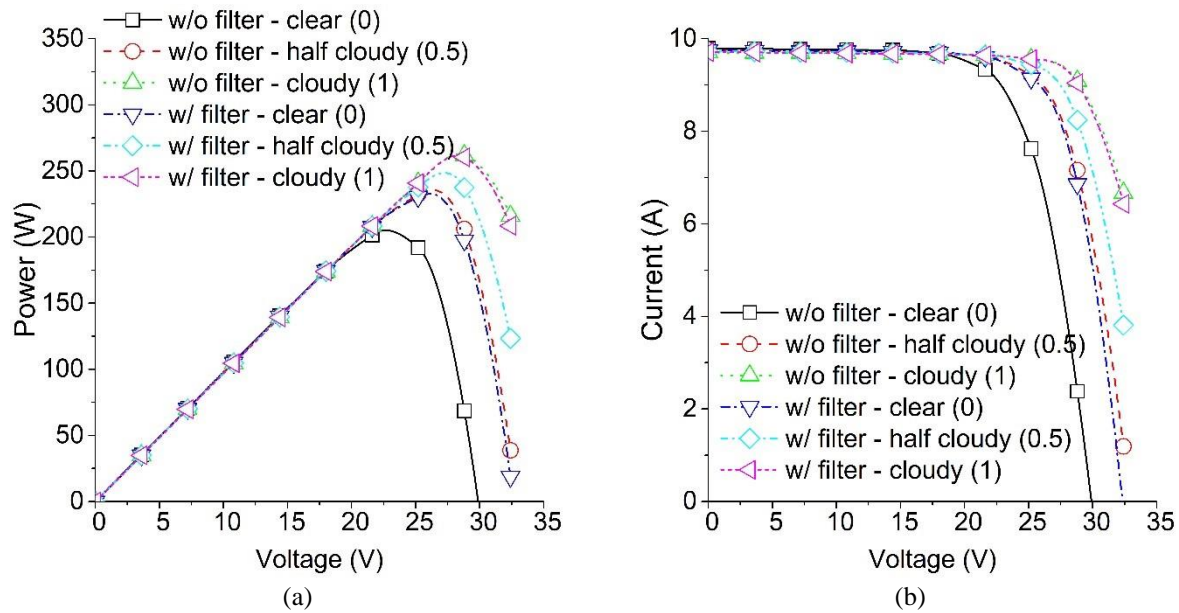
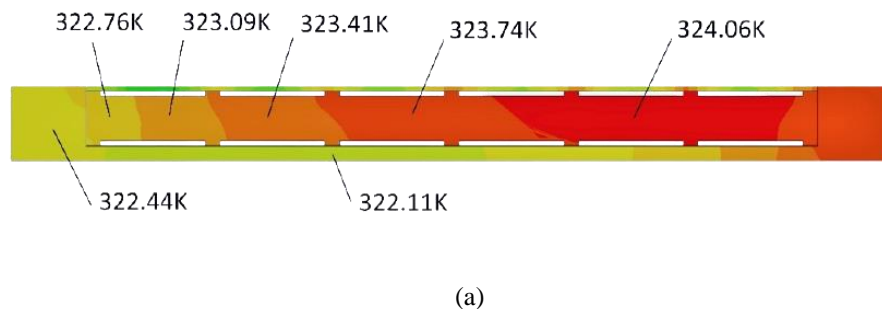


Figure 9. (a) Power-Voltage and (b) Current-Voltage relationships for comparison based on the use of optical bandpass interference filter on different weather conditions

Comparison Between the Maximum Temperature Difference

Overall, it can be seen that the optical bandpass interference filter (visible region) with the antireflective coating (titanium dioxide) is capable of lowering undesired heating in the solar cell. The optical filter with antireflective coating operates by blocking nearly 60% of the unused incident electromagnetic wavelengths from the Sun. Wavelengths that are blocked out by the filter are rays that towards the infrared and ultraviolet regimes. These rays contribute little to energy conversion but lead to a significant increase in the temperature of the solar cell which lowers the cell performance. Solar cells with lower temperature tend to be more efficient, have considerably higher output voltages, and experience negligibly decreases in the electrical currents. These eventually lead to increases in the power outputs of the solar cells. According to the results obtained from MATLAB/Simulink software, the maximum power output of the bare solar panel is 201.53 W while that of the solar panel with the proposed coating and filter is 230.39 W. These results show an increase of 14.3% in the power output, which is relatively significant. This is based on the weather in Kuala Lumpur, Malaysia from 2 to 3 pm, which is typically the hour at which the incident radiant energy from Sun is the most intense. Table 7 depicts the comparison between maximum temperatures in the solar panel with a 3-mm thick optical bandpass interference filter which is in full contact with the glass layer of the solar panel is compared with a conventional solar panel during a sunny day (clear day). The maximum temperature difference observed is nearly 12 K at the end of the hour (Table 8). The temperature difference would definitely vary from hour to hour depending on the orientation of the Sun as well as the intensity of the incident radiation. Figure 10 shows the temperature distributions of the studied solar panel cross-section (a) without and (b) with the coating and filter taking into consideration the directional dependence of the incident solar radiation as well as all modes (conduction, convection, and radiation) of heat transfer around and in the panel. Due to the orientation of the Sun, it can be seen that the right side of the panel is heated more than the left side of the panel. The results obtained are applicable to not only poly-crystalline solar cells but also mono-crystalline solar cells. For thin-film solar cells, different modeling approaches may be required, and they are less likely to be affected thermally because of the minute volumes [26].



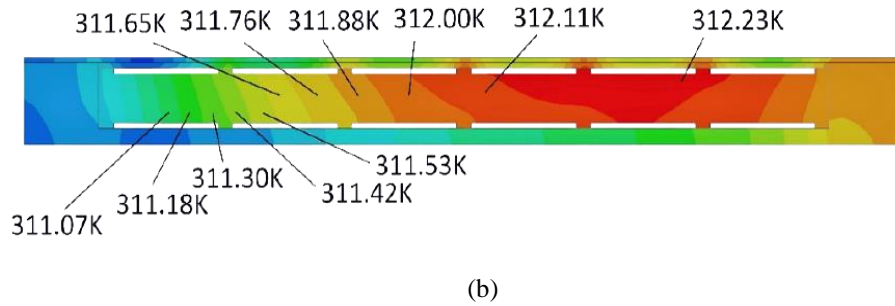


Figure 10. Temperature distribution within the solar panel: (a) without and (b) with the antireflective coating and the optical bandpass interference filter

Table 8. Differences in maximum temperature between unfiltered and filtered solar panel

Time (s)	Type		
	Without Filter (K)	With Filter (K)	Difference (K)
0	300.00	300.00	0.00
600	306.72	303.85	2.86
1200	311.81	306.46	5.35
1800	315.96	308.50	7.46
2400	319.29	310.09	9.20
3000	321.94	311.31	10.63
3600	324.06	312.23	11.83

Cost Effectiveness

As discussed in the results section, a bare solar panel can produce a maximum power output of 201.53 W while that of the solar panel with the proposed coating and filter is 230.39 W. A bare solar panel can produce 588.47 kWh/year while the solar panel with the proposed coating and filter can produce 672.74 kWh/year considering that both panels receive 8 hours of sunlight daily.

According to the tariff provided by Sarawak Energy Berhad, it will cost RM0.29/kWh for the usage of 1 kWh to 500 kWh. A difference of 86.27 kWh/year will result in a saving of additional RM24.44 in the assumption that a household consumes about 500 kWh/month. Table 9 shows the comparison of installation cost and payback in a year. The payback period for a base solar panel is 8.79 years while a modified solar panel takes 10.3 years. It showed that the concept of adding an optical bandpass interference filter with antireflective coating is valid in increasing the performance of the solar cell but not in term of cost-effectiveness.

Table 9. Comparison of the cost of installation and payback in a year

	Base Solar Panel	Modified Solar Panel
Installation Cost (RM)	1500.00	1500.00
Optical Bandpass Interference Filter Cost (RM)	-	430.38
Antireflective Coating Cost (RM)	-	80.00
Electrical Cost Saved/year (RM)	(170.65)	(195.10)
Total	1329.35	1815.28

Justifications of Simulated Results

To our best knowledge, it is difficult to verify the resultant simulation numbers in our settings because of the variations in weather climate as well as different configurations in the design. However, the simulation results can be accessed qualitatively based on previous works in the literature to indicate the validity of our results.

The simulated results were compared with a few relevant research papers. Comparisons were done based on the temperature reduction of the solar cell, current, voltage, power, and the increase in efficiency after the modification to the photovoltaic panel. As mentioned previously in the literature section, Aljoaba, et al. [9] have employed the methods of using active optimal filtering. The predicted temperature of the photovoltaic cell with UV and IR filters is about 3 K lower than that of the conventional panel without a filter. In our simulated results, the larger temperature difference (12K) between the modified and conventional panel can be explained as the cut-off wavelength is narrower (435-720 nm) compared to this research (375-1110 nm). Furthermore, the solar radiation and ambient temperature in the mentioned study were based on the weather conditions in Lexington, Kentucky while our simulation was done in Kuala Lumpur, Malaysia. In addition, the thicknesses of UV and IR filters were not known in the aforementioned work.

Manning and Ewing [27] performed a test to study the effect of window tinting on the temperature of a car. The temperature of the car without tinting was 66.1 °C in 24 minutes, while the temperature of a car tinted with T35 was 61.8 °C in 32 minutes and 59.7 °C using a tinting of T20. These results have proven the ability of a film or filter in reducing the temperature of a material dramatically.

Islam, et al. [28] performed a test on a 250W photovoltaic panel with a constant irradiance of 1000 W/m². The shapes of the I-V curve and P-V curve plotted in the work at different temperatures can be used to justify the results obtained from our MATLAB/Simulink simulation. Both results showed that the solar cell has a higher voltage and power, and a lower current when the operating temperature of the solar cell is lower. The slight difference in the maximum power, current and voltage may be due to the different characteristics of the photovoltaic cell.

Idoko et al. [29] performed a multi-concept cooling technique on a 250W photovoltaic. The multi-concept cooling technique composed of using an Aluminium heat sink at the rear of the module and manual water spraying technique. This technique resembles the solution discussed by increasing the power output through a reduction of the module temperature. An increase of 20.96W can be seen by reducing 8.8K on the module. An increase of $2.38 \frac{W}{K}$ is compared with the increase of $2.44 \frac{W}{K}$ as discussed in this paper, which leads to a percentage difference of 2.52%. The percentage difference may be caused by a difference in the temperature coefficient of P_{max} .

CONCLUSIONS

The use of antireflective coating with optical bandpass interference filter can help to increase the efficiency of a solar panel by reducing the heat on the solar cells. The results are summarized below:

- 1) The optical interference bandpass filter plays the main role of filtering out the unwanted wavelengths while allowing the visible light region to transmit through, whilst the antireflective coating reduces the amount of light reflected from the solar panel thus further increasing the efficiency of the solar panel.
- 2) A reduction of maximum cell temperature by 11.83 K was observed based on the climate in Kuala Lumpur, Malaysia during 2-3 pm when the solar radiation was at its peak hour.
- 3) This reduction in temperature corresponds to a potential 14.32% increase in the maximum cell power output.

The simulated data and results proved the reliability and validity of an optical bandpass interference filter with antireflective coating in reducing unnecessary heats on the solar panel. The reduction of heat on the solar panel not only helps to prolong its life but also improve its performance. These improvements directly translate into cost savings for implementation of solar panels in the global community.

ACKNOWLEDGMENTS

Basil T. Wong is thankful for the support from the Fundamental Research Grant Scheme (FRGS) (Project No. FRGS/1/2018/TK07/SWIN/02/1) funded by the Ministry of Higher Education (MOHE) in Malaysia. The research idea from this work stemmed from the aforementioned funded research project.

REFERENCES

- [1] "BP Statistical Review of World Energy," BP, 2018. Accessed: 20 January 2018. [Online]. Available: <https://www.bp.com/content/dam/bp/business-sites/en/global/corporate/pdfs/energy-economics/statistical-review/bp-stats-review-2018-full-report.pdf>
- [2] L. Fraas, *Low Cost Solar Electric Power*. Springer International Publishing, 2014.

- [3] E. P. Ogberohwo, B. Barnabas, and A. O. Alafiatayo, "Investigating the Wavelength of Light and Its Effects on the Performance of a Solar Photovoltaic Module," *International Journal of Innovative Research in Computer Science & Technology*, vol. 3, no. 4, pp. 61-65, 2015.
- [4] Q. Liu and C. Jia, *Analysis of solar cells in different situations*. Karlskrona, Sweden: Blekinge Institute of Technology, 2015.
- [5] K. Shukla and S. Rangnekar, "A comparative study of exergetic performance of amorphous and polycrystalline solar PV modules," *International Journal of Exergy*, vol. 17, pp. 433-455, 08/24 2015, doi: 10.1504/IJEX.2015.071559.
- [6] K. Sudhakar and T. Srivastava, "Energy and exergy analysis of 36 W solar photovoltaic module," *International Journal of Ambient Energy*, vol. 35, no. 1, pp. 51-57, 2014/01/02 2014, doi: 10.1080/01430750.2013.770799.
- [7] D. M. Tobnaghi, R. Madatov, and D. Naderi, "The Effect of Temperature on Electrical Parameters of Solar Cells," *International Journal of Advanced Research in Electrical, Electronics and Instrumentation Engineering*, vol. 2, no. 12, pp. 6404-6407, 2013.
- [8] W. Beachamp and T. Hart, "UV/IR Reflecting solar cell cover," USA Patent 5449413, 1995.
- [9] S. Z. Aljoaba, A. M. Cramer, and B. L. Walcott, "Active optimal optical filtering of wavelengths for increasing the efficiency of photovoltaic modules," in *2014 IEEE 40th Photovoltaic Specialist Conference (PVSC)*, 8-13 June 2014 2014, pp. 1329-1334, doi: 10.1109/PVSC.2014.6925163.
- [10] I. Roppolo, N. Shahzad, A. Sacco, E. Tresso, and M. Sangermano, "Multifunctional NIR-reflective and self-cleaning UV-cured coating for solar cell applications based on cycloaliphatic epoxy resin," *Progress in Organic Coatings*, vol. 77, no. 2, pp. 458-462, 2014/02/01/ 2014, doi: <https://doi.org/10.1016/j.porgcoat.2013.11.009>.
- [11] C. E. Gouvêa, M. P. Sobrinho, and M. T. Souza, "Spectral Response of Polycrystalline Silicon Photovoltaic Cells under Real-Use Conditions," *Energies*, vol. 10, no. 8, p. 1178, 2017, doi: <https://doi.org/10.3390/en10081178>.
- [12] K. Sudhakar, N. Jain, and S. Bagga, "Effect of color filter on the performance of solar photovoltaic module," in *2013 International Conference on Power, Energy and Control (ICPEC)*, 6-8 Feb. 2013 2013, pp. 35-38, doi: 10.1109/ICPEC.2013.6527620.
- [13] W.-J. Ho, J.-C. Lin, J.-J. Liu, W.-B. Bai, and H.-P. Shiao, "Electrical and Optical Characterization of Sputtered Silicon Dioxide, Indium Tin Oxide, and Silicon Dioxide/Indium Tin Oxide Antireflection Coating on Single-Junction GaAs Solar Cells," *Materials*, vol. 10, no. 7, p. 700, 2017, doi: <https://doi.org/10.3390/ma10070700>.
- [14] V. K. Jain and A. P. Kulshreshtha, "Indium-Tin-Oxide transparent conducting coatings on silicon solar cells and their "figure of merit"," *Solar Energy Materials*, vol. 4, no. 2, pp. 151-158, 1981/01/01/ 1981, doi: [https://doi.org/10.1016/0165-1633\(81\)90038-1](https://doi.org/10.1016/0165-1633(81)90038-1).
- [15] M. Ciobanu, J. P. Wilburn, M. L. Krim, and D. E. Cliffel, "1 - Fundamentals," in *Handbook of Electrochemistry*, C. G. Zoski Ed. Amsterdam: Elsevier, 2007, pp. 3-29.
- [16] R. Kishore, S. N. Singh, and B. K. Das, "PECVD grown silicon nitride AR coatings on polycrystalline silicon solar cells," *Solar Energy Materials and Solar Cells*, vol. 26, no. 1, pp. 27-35, 1992/03/01/ 1992, doi: [https://doi.org/10.1016/0927-0248\(92\)90123-7](https://doi.org/10.1016/0927-0248(92)90123-7).
- [17] K. Seshan, *Handbook of Thin Film Deposition*. William Andrew, 2012.
- [18] H. Bellia, R. Youcef, and M. Fatima, "A detailed modeling of photovoltaic module using MATLAB," *NRIAG Journal of Astronomy and Geophysics*, vol. 3, no. 1, pp. 53-61, 2014/06/01/ 2014, doi: <https://doi.org/10.1016/j.nrjag.2014.04.001>.
- [19] P. S. Paul, S. Mondal, N. Akter, and S. M. Mominuzzaman, "Modeling combined effect of temperature and irradiance on solar cell parameters by MATLAB/ simulink," in *8th International Conference on Electrical and Computer Engineering*, 20-22 Dec. 2014 2014, pp. 512-515, doi: 10.1109/ICECE.2014.7026896.
- [20] H. Ibrahim and N. Anani, "Variations of PV module parameters with irradiance and temperature," *Energy Procedia*, vol. 134, pp. 276-285, 2017/10/01/ 2017, doi: <https://doi.org/10.1016/j.egypro.2017.09.617>.
- [21] B. Swatowska, T. Stapinski, K. Drabczyk, and P. Panek, *The Role of Antireflection Coatings in Silicon Solar Cells – The Influence on Their Electrical Parameters*. 2011, p. 487.
- [22] D. K. Pandey, R. B. Lee, and J. Paden, "Effects of atmospheric emissivity on clear sky temperatures," *Atmospheric Environment*, vol. 29, no. 16, pp. 2201-2204, 1995/08/01/ 1995, doi: [https://doi.org/10.1016/1352-2310\(94\)00243-E](https://doi.org/10.1016/1352-2310(94)00243-E).
- [23] Y. A. Cengel and A. J. Ghajar, *Heat and mass transfer : fundamentals & applications*. (in English), 2015.
- [24] M. Hammami, S. Torretti, F. Grimaccia, and G. Grandi, "Thermal and Performance Analysis of a Photovoltaic Module with an Integrated Energy Storage System," *Applied Sciences*, vol. 7, no. 11, 2017, doi: 10.3390/app7111107.
- [25] D. Rajput, "Effect Of Dust On The Performance Of Solar PV Panel," *International Journal of ChemTech Research*, vol. 5, pp. 1083-1086, 03/15 2013.
- [26] J. Adeeb, A. Farhan, and A. Al-Salaymeh, "Temperature Effect on Performance of Different Solar Cell Technologies," *Ecological Engineering*, vol. 20, pp. 249–254, 05/01 2019, doi: 10.12911/22998993/105543.
- [27] R. Manning and J. Ewing, "Temperature in Cars Survey," RACQ Vehicle Technologies Department, 2009.
- [28] M. A. Islam, A. Merabet, R. Beguenane, and H. Ibrahim, "Modeling solar photovoltaic cell and simulated performance analysis of a 250W PV module," in *2013 IEEE Electrical Power & Energy Conference*, 21-23 Aug. 2013 2013, pp. 1-6, doi: 10.1109/EPEC.2013.6802959.
- [29] L. Idoko, O. Anaya-Lara, and A. McDonald, "Enhancing PV modules efficiency and power output using multi-concept cooling technique," *Energy Reports*, vol. 4, pp. 357-369, 11/01 2018, doi: 10.1016/j.egy.2018.05.004.